

THE ROLE OF BATTERIES IN NEAR-FUTURE ENERGETICS

*Slavko Mentus**

Serbian Academy of Sciences and Arts, Knez Mihajlova 35,
Belgrade 11000, Serbia

Abstract: Since the first oil crisis in early 70-ties, the electrochemists strive to develop a chemical power source able to replace the liquid fossil fuels in traffic. Noticeable success was achieved in the decade 1980-1990. Thanks to a new class of materials – intercalate compounds, a new battery called lithium-ion battery was commercialized, having much higher energy density than its predecessors. In this work the origin of its high energy density is explained. The emergence of new battery supported effectively the expansion of use and the development of portable electronics - mobile phones, lap-top calculators tablets etc. Since 2010, connected to the global intentions to prevent climate changes, the batteries received the role of the energy sources of electric cars. Recently, connected to the rising use of renewable energy sources known to suffer of changeable intensity, batteries take also the role of grid energy storage, having the function to smooth the disturbances in grid voltage. All this caused huge rise in batteries usage, and poses the question about the availability of global resources of lithium, cobalt and nickel needed for battery production. The recent forecast is that these resources will be exhausted very soon in the decade 2030-2040. Thus, there is a strong need to search for new battery types, to maintain, at least partly, available lithium resources for more demanding applications. As a part of solutions having real perspective, the development of sodium-ion battery is currently in progress. In that sense, some perspective anode and cathode materials were considered.

Keywords: climate changes; intercalate compounds; Li-ion battery; metal resources; Na-ion battery.

1. HISTORY OF LITHIUM-ION BATTERIES – FROM THE DISCOVERY TO THE NOBEL PRICE FOR INNOVATION

Batteries are portable chemical reactors which convert the energy of redox chemical reactions directly into electric energy practically without any losses. The secondary batteries may be charged upon discharging, and are labeled as rechargeable ones. Thanks to their long working life, rechargeable batteries are more desirable from the point of economy and environmental protection than the primary ones. The classical secondary batteries, lead-acid one, discovered in 1859., and the nickel-cadmium one discovered in 1900., have been more than one century in commercial use and reached saturation of any advancements far ago.

Main battery characteristics is practical specific energy (practical energy density). It may be derived from coulombic capacity of either cathode or anode material, which is the product of molar coulombic capacity ($z \times 26,8$ Ah, z = oxidation

number) and number of moles n incorporated in a battery, i.e.:

$$\text{Coulombic capacity} = n_{a(c)} \times (z \times 26,8) \text{ Ah}$$

This quantity denotes the quantity of electricity (Ah) which may be obtained from a charged battery.

The practical energy density is a product of coulombic capacity of either cathode or anode material (being mutually equal), and voltage ε , divided by the sum of masses of cathode and anode materials and all other construction parts (current collectors, separators, contacts, housing) making battery practically usable:

$$\text{Practical energy density Wh/kg} = \frac{n_{a(c)} \times z \times 26,8 \times \varepsilon}{n_a M_a + n_c M_c + \sum M_{constr}}$$

Obviously, high voltage and low masses of reactants and construction parts are desirable for high practical energy density.

Since classical batteries use aqueous electrolyte solutions, their voltage is limited to around 1.5 V. Namely water suffers of electrolytic

* Corresponding author: slavko@ffh.bg.ac.rs

decomposition at higher voltages, and this, together with a high molar masses of reactants, restricts the advance in their energy density over actually achieved 35-45 Wh/kg.

The first oil crisis in 1970-ties impelled electrochemists to search for new battery types, richer in energy from classical ones, able to replace oil as a power source in the automobiles. Some initial success was achieved with high-temperature batteries with molten salts or ionically conducting solids as electrolytes, such as LiAl / LiCl, KCl / FeS_x, and Na / beta-Al₂O₃ / S, working at ~ 300 °C [1] but they were impractical for non-stationary devices.

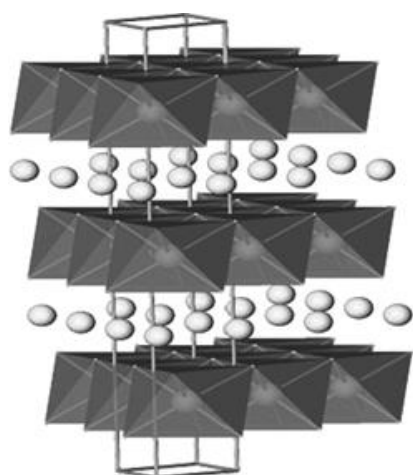


Figure 1. The structure of lithiated titanium disulphide

Noticeable success was achieved in the decade 1980-1990. Thanks to the discovery of a new class of materials – so called intercalate compounds, a new battery type, called lithium-ion battery was commercialized, having multiple higher energy density than its predecessors.

In intercalate compounds we distinguish two reactants, one called host or hosting material and the other called guest or guesting material. In early discovered intercalates, hosting material was a solid compound of layered crystal structure. Inside layers the structure units: atoms or atomic groups, are bonded by strong either covalent or ionic bonds, while the layers are mutually bonded by weak van der Waals forces. Such a structure, upon application of any activation energy, mostly by heating, allows the guest atoms and molecules to react chemically, in a way the guest atoms penetrate between the layers of hosting material occupying regular crystallographic positions. This type of reaction, called intercalation reaction, leads to the crystallographically ordered compounds with particular physicochemical behavior in comparison to the reactants, i.e. with somewhat modified dimensions of elemental cell, as well as with

modified ionic or electronic conductivity and chemical reactivity.

First intercalate compounds were discovered in 1938. Namely, Rüdorff et al. [2] by heating graphite with sulphuric acid or bromine, obtained the so called graphite salts, with molecules of sulphuric acid or bromine incorporated between graphene layers. Some time later Herold [3] obtained intercalate compound KC₈ by heating graphite with potassium in a closed vessel. This compound was golden-brownish in color and displayed higher electronic conductivity than graphite and lower reactivity with water than metallic potassium.

Rüdorff et al. [4] discovered later that some layered halcogenides of transition metals may build intercalates with alkali metals, if heated in organic solutions of alkali metals. As an example, Figure 1. shows the structure of the compound obtained by reaction of titanium disulphide and lithium. The basic structure units are the layers of interconnected polyhedral units with titanium ions in centers and oxygen ions in corners. Lithium ions presented by spheres are incorporated between the layer of hosting TiS₂, causing a small enlargement of interlayer distance. Whittingham [5] constructed a battery composed of lithium anode and TiS₂ as cathode, in an aprotic organic electrolyte solution (Figure 2). The connection of electrodes starts discharging process, when lithium anode liberated

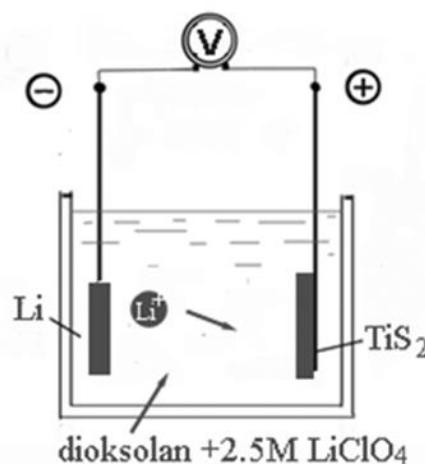
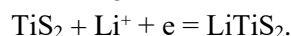


Figure 2. The sketch of Whittingham's battery Li/TiS₂

lithium cations into electrolyte and electrons into metallic part of electric circuit. On the cathode the following reaction occurs:



Simultaneously with the incorporation of lithium ions between TiS₂ layers, electrons liberated at anode reduce Ti⁴⁺ ions to Ti³⁺ state, which keeps the electroneutrality of LiTiS₂. This battery operated

within 1.5 to 2.5 V window (Figure 3). It evidenced that intercalate materials may be formed electrochemically, and indicated a way how to use lithium as an active material of rechargeable batteries.

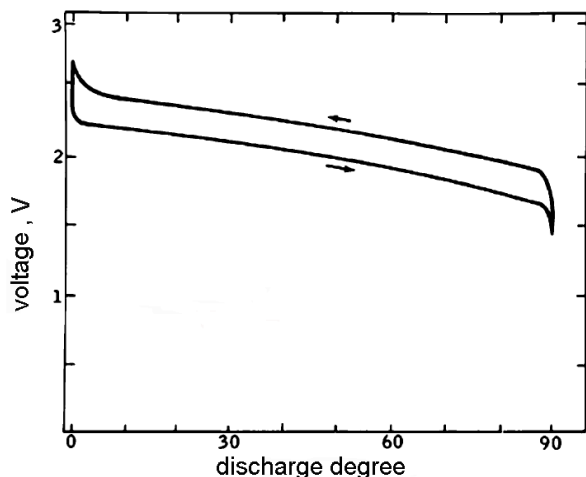


Figure 3. The dependence of voltage of Li/LiTiS₂ battery on the degree of discharge during galvanostatic charging/discharging

Important advance was achieved by the group of professor J. Goodenough in the decade 1980-1990 [6–9]. Namely, they published that the layered oxides of transition metals may build intercalate compounds with lithium, which have much higher positive potential than TiS₂ relative to metallic lithium. The synthesis consisted simply in heating intimate mixture of thermodegradable salts (for instance hydroxides, carbonates or nitrates) of lithium and transition metal. For instance layered compound LiCoO₂ spinel LiMn₂O₄ [6] and layered compound LiNiO₂ [7,8] displayed roughly 4 V relative to metallic lithium [9]. Therefore, LiCoO₂ arranged as cathode material as shown in Figure 2, gave more energetic battery, with the theoretical energy density of 1.11 kWh kg⁻¹. In 1997. Goodenough's group published the discovery of new intercalate compound LiFePO₄, of olivine structure, which displayed ~3.7 V versus metallic lithium, somewhat lower than predecessors, however, its significance was in high abundance of chemicals needed for synthesis and in high environmental friendliness [10].

The intercalates discovered by Goodenough's group displayed various dimensionality of Li-ion diffusion (Figure 4) [11] Lithium ions may diffuse through the crystal either in only one direction, along the one-dimensional channels as in the case of olivine LiFePO₄, or in two directions along the planes of lithium sites, as in the case of layered oxides LiCoO₂ and LiNiO₂, or in even three

directions, along the three-dimensional channels through the crystals, as in the case of spinel LiMn₂O₄.

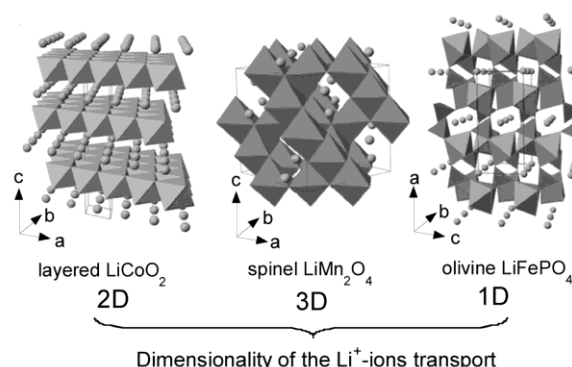


Figure 4. The crystal structures of intercalates discovered by Goodenough's group, displaying one-, two- and three-dimensional diffusion of Li ions. [11]

Main obstacle in elaboration of a practically usable rechargeable battery originated from the lithium anode. It was too reactive with each of potential electrolyte solvent, and during successive cathodic depositions, lithium deposited in form of dendrites which easily fell off from anode bulk causing low current efficiency. Further to this, dendrites penetrate through separator and make internal short-circuits, causing local overheating and danger of battery self-ignition. Both material loss and internal short-circuiting caused short cycling life of batteries with metallic lithium anode. An important advancement in solving anode problem presents the discovery by Yazami [12], that lithium may be intercalated into graphite electrochemically to the content corresponding to the composition LiC₆. Due to a larger molar mass of LiC₆ relative to Li (79 g against 7 g) the coulombic capacity is more than tenfold lower, amounting to 370 mAh g⁻¹ (versus 3800 mAh g⁻¹ for pure Li) but its potential is somewhat higher than zero, and suppress the deposition of metallic lithium, thus this anode is much more safe than metallic lithium and enables much higher cyclic life of the battery.

Utilizing the experience of Goodenough and Yazami, Akira Yoshino solved almost all commercialization problems of Li-ion battery, involving the solutions for separator, electrolyte and current collectors supporting the electrode materials. According to his first patent [13], a particular carbon type („petroleum coke”) was used as anode material, LiCoO₂ as cathode, Cu foil as the anode current collector, Al foil as the cathode current collector, and LiPF₆ dissolved in propylene carbonate as electrolyte (Figure 5). In an additional patent Yoshino [14] introduced porous polyethylene foil as

a separator permeable for electrolyte (Figure 6). This enhanced the safety of battery against explosion. Namely, if an internal short-circuit occurs, local jump of temperature melts the plastic membrane and cuts further current, preventing eventual fire and explosion.

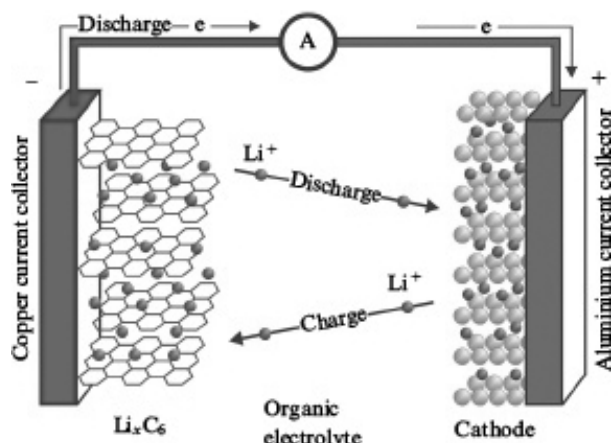


Figure 5. Battery $\text{LiC}_6/\text{LiCoO}_2$. First Li-ion battery according to the Yoshino patent [13]

LiCoO_2 intercalate through electrolyte, accompanied by electron transfer through metal conductors in the same direction, according to the chemical reaction:

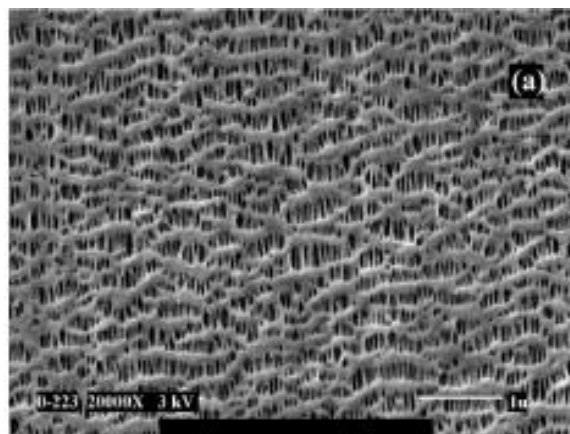
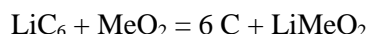


Figure 6. Microphotograph of a porous polyethylene separator of lithium ion battery. The length of the white mark is $1 \mu\text{m}$

The battery works simply transferring lithium ions from graphite intercalate into the Li-deficient

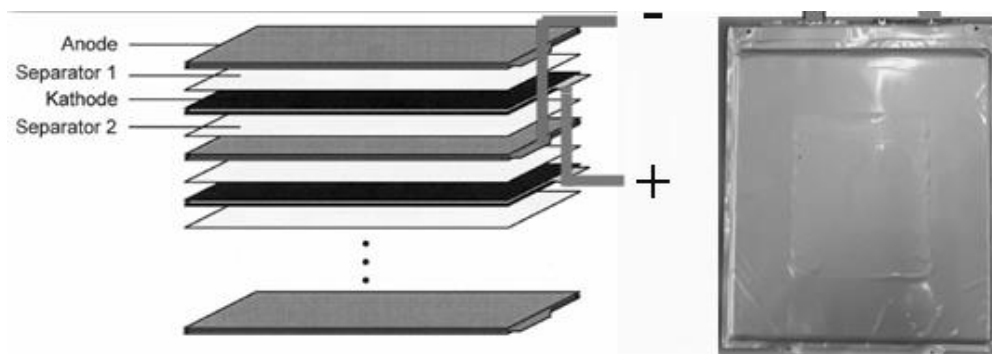


Figure 7. The stacking of the cathode, anode and separator foils and their packing into evacuated prismatic plastic housing.

The electrolyte serves only to transport lithium ions between anode and cathode materials. Therefore, its use may be limited only to that amount sufficient to soak electrode materials and separator. Thin layer appearance of anode, cathode and separator (Figure. 7) enabled the space economy and dense packing of battery components either in cylindrical or flat stacked forms. Early in 1990s, on the basis of Yoshino patents, three companies started production of lithium ion batteries: Sony Energytec. Inc., C/LiCoO_2 , Moli Energy Ltd., C/LiNiO_2 [15] and Bell Communication Research (Bellcore) $\text{C}/\text{LiMn}_2\text{O}_4$ [16].

Significantly lower molar masses of cathode and anode materials than those of lead-acid battery, and/or higher voltage from its precedents (see the

Table 1) as well as negligible amount of electrolyte enabled about four times higher practical energy density of Li-ion battery. Novel batteries thus occupy gradually rising part of battery market, and generally influence the life. The scientists most distinguished in its development, S. Whittingham, J. Goodenough and A. Yoshino were awarded by Nobel prize in chemistry in 2019.

Many researchers invested effort to improve practical energy density, charging rate and cycle life of Li-ion batteries. Liu et al [17] found that and rhombohedral $\text{Li}(\text{Ni}_y\text{Mn}_z\text{Co}_{1-y-z})\text{O}_2$ (usually abbreviated as NMC) (space group $R\bar{3}m$) where y and z can vary between 0 and 1 eliminates particular disadvantages of simple oxide components. Ohzuku et al [18] recommended $\text{LiNi}_{0,33}\text{Mn}_{0,33}\text{Co}_{0,33}\text{O}_2$ as an

optimal cathodic material. Later, with intention to save relatively expensive cobalt, Ni-rich compositions were proposed, such as $\text{LiNi}_{0.70}\text{Co}_{0.15}\text{Al}_{0.15}\text{O}_2$ [19,20] (abbreviated in the

literature as NCA). All these materials display structural stability, higher specific energy and extended cycle life and are today the usual cathode materials of all-purpose Li-ion batteries [21–23]

Table 1. The cathode and anode materials, electrolytes, voltage, theoretical and practical energy density of classical (lead-acid, and alkaline Ni-Cd) and contemporary (Li-ion) batteries variances

Type	anode	cathode	electrolyte	voltage (V)	Wh kg ⁻¹ Theor.	Wh kg ⁻¹ Practic.	Wh l ⁻¹ Practic.
Pb/PbO ₂	Pb	PbO ₂	H ₂ SO ₄	2.0	252	35	70
Cd-Ni	Cd	NiOOH	KOH	1.2	244	50	75
Li-ion	LiC ₆	Li _x CoO ₂ 0.6e	EC/DMC + LiPF ₆	3.7	420	206	530
Li-ion	LiC ₆	LiMn ₂ O ₄ 0.8e	EC/DMC + LiPF ₆	3.8	330	132	340
Li-ion	LiC ₆	LiNi _{0.33} Co _{0.33} Mn _{0.33} O ₂ 0.7e	EC/DMC + LiPF ₆	3.6	450	210	530
Li-ion	LiC ₆	LiNi _{0.8} Co _{0.15} Al _{0.05} O ₂ 0,75e	EC/DMC + LiPF ₆	3.6	470	265	690

$\text{LiNi}_{0.6}\text{Mn}_{0.2}\text{Co}_{0.2}\text{O}_2$ (NCM series) and $\text{LiNi}_{0.8}\text{Co}_{0.15}\text{Al}_{0.05}\text{O}_2$ (NCA series) are commonly used cathodic materials in contemporary automobile batteries. In the period 2011-2090 Serbian Ministry of Education, Science and Technological development financed the project entitled Lithium-ion batteries and fuel cells-research and development, within of which Serbian scientists contributed significantly to the expanding of science and practice of alkali-ion batteries [24–29].

2. CONTEMPORARY APPLICATIONS OF LITHIUM-ION BATTERIES: THE THREE BIG ROLES CHANGING EVERYDAYS LIFE

Li-ion batteries are applied in consumer electronics and communications (mobile phones, tablets, lap-top computers), transportation (hybrid-electric vehicles, plug-in hybrid electric vehicles, and pure electric vehicles) implantable medical devices (Neuro-stimulators, pacemakers, defibrillators), aerospace, defense, toys etc. Up to 2020, only 20 years upon appearance, the Li-ion market increased up to ~\$8-10 billion.

The emergence of new battery contributed significantly to the development of mobile phones, lap-top calculators and other portable electronics. Presently, mobile phone is a usual personal gadget of a contemporary men, and lap-top computers is an unavoidable mate of every educated person. In 2010

portable electronics was the main consumer of battery energy, using 21 GWh (gigawatt hours) per year. The perspective is it will consume 45 GWh in 2020. From 2010., batteries are given a second big role, as a power source of electric cars. Namely, after rigorous alerts of scientists about rising danger of climate changes caused by abrupt rise of consumption of fossil fuels and consequent rise in CO₂ concentration in atmosphere, the Organization of United Nations (OUN) decided to limit gradually the emission of CO₂ to a sustainable level by 2050. A part of this decision was the replacement of oil powered vehicles by electric vehicles. Since the price of Li-ion batteries became acceptable, from 2010 the vehicles powered by Li-ion batteries appeared in regular traffic.



Figure 8. Tesla electric car with its battery pack

In order to estimate the energy of batteries needed for replacement of oil powered cars by electric ones, we may start with the fact that average

oil powered automobile consumes roughly 8.6 dm^3 of liquid fossil fuel (gasoline or oil) per 100 km. The combustion energy of fossil fuel is $\sim 33.8 \text{ MJ dm}^{-3}$ what is equal to $\sim 9400 \text{ kWh dm}^{-3}$. For a 500 km range of autonomy, usual for a contemporary car, the energy of $\sim 404000 \text{ kWh}$ of fossil fuel is needed. Calculating with 25% efficiency of an internally combusting engine, this means that average automobile consumes effectively $\sim 100 \text{ kWh}$ of kinetic energy for an autonomy range of 500 km, or 20 kWh for 100 km autonomy range, while 75% of energy is lost as heat.

Assuming that practical electric energy of a battery may be converted in kinetic energy almost without any losses, and that (see Table 1) practical energy density of a contemporary battery is roughly 200 kWh kg^{-1} , one can easily calculate that the battery containing 1kWh of energy weights $\sim 5 \text{ kg}$. That means, a contemporary automobile needs $\sim 500 \text{ kg}$ of batteries to dispose with 100 kWh of energy enabling the autonomy range of 500 km.

Today only Tesla company produces electric cars with autonomy range 500 km, requiring battery pack of 100 kWh (Figure 8). Majority of automobile producers, accounting with the statistical data that an average daily travel distance of an urban driver is $\sim 50 \text{ km}$ only, incorporate battery packs enabling distance ranging 100-160 km, requiring battery packs containing 16-40 kWh of energy, having mass of 100 - 200 kg, which are commensurably cheaper.

In 2017 the number of electric vehicles produced worldwide exceeded one million, and an exponential rise is expected in future. The total energy containing in automobile batteries increases rapidly from approx. zero in 2010 to 76 GWh/year in 2010, with prediction to amount to 245 GWh/year in 2030. The third important contemporary role of lithium-ion batteries are connected to the rising use of solar and wind energy. Here the batteries take the role of grid energy storage, to smoothen the

disturbances in grid supply. Formerly lead acid and nickel-cadmium batteries were used in that sense, however, today lithium-ion batteries compete effectively in this part of battery market. For instance, in 2018 the company Tesla installed a big wind-generator stabilization station within an Australian field Hornsdale Power Reserve (Figure 9).



Figure 9. Grid stabilisation station Hornsdale Power Reserve, Australia.

A complete device, based on Samsung batteries, provides installed energy of 129 MWh and power 100 MW, and serves to stabilize grid output power in the case of drop in wind power or other problems in energy supply. A part of power in amount 70 MW may maintain local energetic system during 10 minutes, and a part of remaining 30 MW may maintain energetic system stable during three hours. Presently grid stabilization stations are not great battery consumer (see Table 2) however its rise is predicted to an energy amount of 10 GWh in 2025 and 30 GWh in 2030. The Table 2 [30] summarizes the demands in li-ion battery energy of main energy consumers: portable electronics, electric vehicles and grid energy storage stations, both in past and predicted for the near future.

Table 2 The rate of battery energy consumption in GWh per year, during the last decade and the prediction for the next one [30]

	2010	2015	2020	2025	2030
Portable electronics (mobile phones, tablets, cameras, lap-top computers)	21	31	45	66	100
Electric vehicles (all types)	0	13	76	137	245
Grid energy storage stations	0	0	2	10	30
Other applications	1	1	2	7	15
Total	22	45	125	220	390

3. FORECAST OF DEFFICIENCIES OF RAW MATERIALS FOR Li-ION BATTERIES PRODUCTION

The rising amounts of various metals consumed by battery producers states the question of their global availability. The concern relates primarily to lithium, cobalt and nickel having in mind their low abundance in Earth crust.

Neglecting the fraction dissolved in oceans unavailable due to very low concentration, the global reserves of lithium bounded in minerals are estimated to 47 million tons. However only 14 million tons may be extracted economically. In 2016., 37800 tons of lithium metal are produced, 39% or ~ 14700 tons of which are consumed in battery production [30].

Global reserves of nickel are 78 million tons, and world annual production in 2016 amounted to 2250000 tons. Cobalt reserves are estimated to amount to 7 million tons while annual production in 2016 was 123000 tons, of which 37000 tons are used for batteries.

According to the battery chemistry, and average energy density shown in Table 1, said to be 200 Wh kg^{-1} , one may account with the consumption of 0.160 kg of Li, 0.06-0.12 kg of Co (0.1 kg in average) and 0.4 kg of Ni per 1 kWh of battery energy. These amounts multiplied, for instance, by one hundred are needed for Tesla highest range battery pack.

According Yushin, Nature [31], car manufacturers predict that 10 - 20 million electric cars per year will be produced around 2025. If on the basis of battery chemistry, each car battery requires 10 kg of cobalt, by 2025, electric vehicles would need 100,000–200,000 tons of cobalt per year rhombohedral - close to the global current production. Accordingly, 400,000–800,000 tons of nickel would be required annually, what present a percentage of 20 – 40% of this metal presently used.

By 2050, a planned production rate of 50 - 80 million electric vehicles per year would require 500,000–800,000 tons of cobalt. This will exceed current mining capacities already beyond 2030. In addition, 2–3 times more nickel would be needed by 2050. One may easily see that the shortages in nickel would arise by the mid-2030s. One may expect that demand will outstrip metal production even sooner if trucks, buses, aeroplanes and ships would become powered by batteries.

Accounting with the consumption of 16 kg of Li per one 100 kWh battery pack, up to the end of 2030, car producers will need roughly 400,000 tons of Li which is 2.9 % of global resources.

According to a Japanese report published in 2010, [32] about 7.9 million tons of metallic Li will be required when 50% of the oil-driven cars in the world are replaced by XEVs (including hybrid EVs (HEVs) and plug-in hybrid electric vehicles (PHEVs)). Obviously one needs to consider urgently the ways either to decelerate the consumption of raw materials of Li-ion for batteries or to develop batteries based on other raw materials.

4. HOW TO OVERRUN THE DEFFICIENCY OF RAW MATERIALS FOR Li-ION BATTERIES? SODIUM-ION BATTERIES AS A REAL ALTERNATIVE

The life of resources of materials for lithium-ion batteries may be prolonged by excluding critical elements, cobalt and nickel, from battery production. In this way development of lithium-air (theoretical energy density 13200 Wh/kg) and lithium-sulfur (theoretical energy density 2600 Wh/kg) batteries is in progress. The prediction is that practical energy density of 900 Wh/kg for Li-air and $\sim 600 \text{ Wh/kg}$ for Li-S batteries may be achieved [33]. In addition, this would substantially decelerate the consumption of lithium resources, and prolong the period of their availability.

However, many problems have to be resolved to achieve production of Li-air or Li-sulphur batteries on a commercial level. Thus in continuation of this study a way which does not account with the use of lithium at all will be considered. This new way is the development of sodium-ion batteries. Sodium (Na) stays below Li in the periodic table and thus both these elements behave similarly in the sense of chemical properties. The Sodium-ion batteries operate similarly to lithium-ion batteries, i.e., the alkali ions exchange positions between the anode and the cathode during charging and discharging procedure. Accounting with a relatively unlimited abundance, and low price of raw materials, the development of sodium -ion batteries is in progress and close to commercialization

The investigations published thus far revealed that many compounds able to intercalate lithium are also able to intercalate sodium. Figure 10 shows the range of voltage during intercalation reactions versus achievable coulombic capacity for the intercalation materials able to exchange sodium ions known up to 2013 [34].

Usually, due to a higher ionic radius of sodium versus lithium cations, the diffusion of

sodium ion is slower than lithium ion, thus sodium intercalate materials show lower rate performance than lithium ones. Also, mean potential of sodium

intercalates is lower than lithium intercalate ones, what means lower energy density. Presently sodium ion batteries may not compete to the lithium-ion batteries.

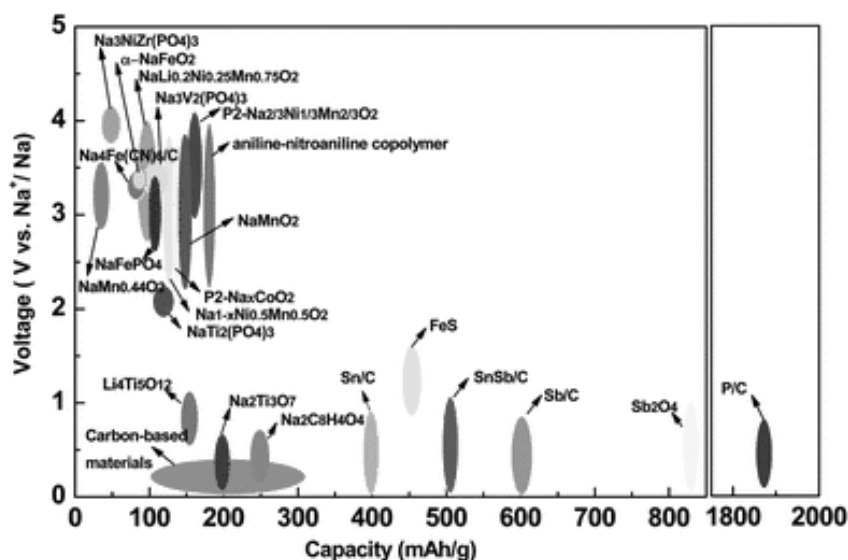


Figure 10. The voltage capacity relationship of various materials for either anodes or cathodes of Na-ion batteries – survey made in 2013 [34] Copyright The Royal Society of Chemistry 2013

However, many battery applications do not require highest rate or energy performances, for instance grid stabilization units. Apart of this, it is not impossible that the performance of sodium-ion batteries may become very close to those lithium-ion ones, and consequently replace them completely on the battery market.

In continuation, some studies of perspective cathode and anode materials of sodium-ion batteries will be considered. Among cathode materials, those displaying 3D diffusion of alkali ions are considered, since such materials enable the highest diffusion coefficients and fastest charging/discharging rates.

5. CATHODE MATERIALS OF SODIUM-ION BATTERIES

Prussian blue analogs

The Prussian blue (hexacyanoferrate) analogs present a group of perspective cathode materials for sodium ion batteries. Prussian blue analogs (PBAs) generally have the composition $\text{Na}_x\text{M}_2[\text{M}_1(\text{CN})_6]_y \cdot n\text{H}_2\text{O}$ (x being limited between 0 and 2, and y being limited between 0 and 1), where M_1 and M_2 are transition metal such as Mn, Fe, Co, Cu etc. [35]. Most of PBAs are cubic phases with 6-fold coordination of MII,III- O_6 octahedra. The CN groups interconnect the ions of transition metals

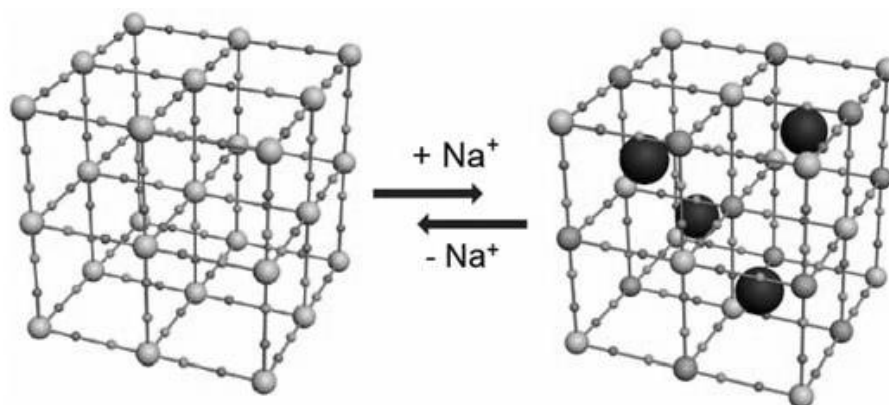


Figure 11. Prussian blue crystals $\text{Na}_x\text{Fe}[\text{Fe}(\text{CN})_6]$, empty of sodium ions (charged state) (Left), and with partly filled sodium ion sites (partly discharged state). The three-dimensional diffusion is allowed [36]. Copyright: The Royal Society of Chemistry 2014

making basic crystal framework (Figure 11). You et al [36] synthesized Na-enriched Prussian blue, $\text{Na}_{1+x}\text{Fe}^{\text{III}}[\text{Fe}^{\text{II}}(\text{CN})_6]$ as a solid precipitate, when a solution of ferric salt is added under stirring to a solution of $\text{Na}_4\text{Fe}(\text{CN})_6$. Its crystal structure is cubic, with sodium ions inserted into the free sites within three-dimensional Na^+ migration pathways. Low diffusion energy barriers for sodium ions enable fast diffusion of 3D type, and consequently, fast intercalation/deintercalation reactions. The modifications of chemical compositions by insertion or deinsertion of alkaline cations does not influence the overall crystalline structure. Both ferrous and ferric ions, by a change of oxidation number, participate in the redox reactions accompanying intercalation/deintercalation processes, in order to maintain electroneutrality of solid phase.

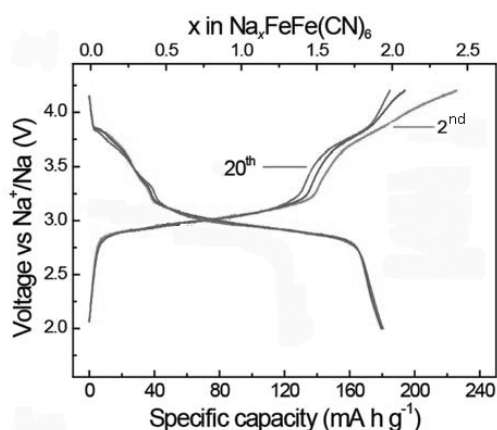


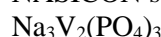
Figure 12. Galvanostatic charging/discharging curve (2nd, 5th and 20th cycle) of $\text{Na}_x\text{Fe}[\text{Fe}(\text{CN})_6]$ in 1 M NaPF_6 in EC and DEC at 1:1 volume ratio, [36] Copyright: The Royal Society of Chemistry 2014

In the organic electrolyte solution composed of 1 M NaPF_6 dissolved in ethylene carbonate (EC) and diethyl carbonate (DEC) at 1:1 volume ratio, You et al [36] found that this material displays high specific capacity of 170 mAh g^{-1} , with the mean voltage close to 3 V versus metallic sodium, without apparent capacity loss after 150 cycles (Figure 12).

Xiao et al, [37] studied the structural evolution of a $\text{Na}_2\text{FeMn}(\text{CN})_6$ cathode upon Na intercalation. They concluded that maximum two Na^+ ions per formula unit may be incorporated if both the M1 and the M2 transition metal elements may accommodate their oxidation state leading to a theoretical specific capacity of 170 mAh/g . This was practically proved by Shen et al [38] These authors synthesized sodium manganese hexacyanoferrate $\text{Na}_x\text{MnFe}(\text{CN})_6$ as a solid precipitate, starting with the aqueous solution of sodium hexacyanoferrate ($\text{Na}_4\text{Fe}(\text{CN})_6 \cdot 10\text{H}_2\text{O}$), manganese sulfate monohydrate ($\text{MnSO}_4 \cdot \text{H}_2\text{O}$), sodium chloride (NaCl) and sodium citrate dihydrate

($\text{Na}_3\text{C}_6\text{H}_5\text{O}_7 \cdot 2\text{H}_2\text{O}$). The solid precipitate was separated and dried. On galvanostatic charging/discharging experiments, the product displayed almost flat galvanostatic charging/discharging plateau at mean voltage 3.6 V vs sodium metal. The galvanostatic charging/discharging curves indicated large coulombic capacity of 144 mAh g^{-1} under a 0.1 C rate, good rate performance (115.6 mAh g^{-1} under a 1 C rate, 86.6 mAh g^{-1} under a 10 C rate), and good cycling stability (73.4% retention after 780 cycles under a 0.5 C rate, and 72.7% retention after 2100 cycles under a 1 C rate).

NASICON structures



Bui et al [39] reported that $\text{Na}_3\text{V}_2(\text{PO}_4)_3$ (NVP) appears in a rhombohedral NASICON structure, displayed in Figure 13. This structure assumes three-dimensional framework built of $[\text{V}_2(\text{PO}_4)_3]$ units, created by corner-sharing of VO_6 octahedra and PO_4 tetrahedral along the c-axis direction. The corner-sharing three VO_6 octahedra and three PO_4 tetrahedra build the hexagonal narrow passages, the shortest diameter of which equals roughly twice the sum of the Na^+ and O^{2-} ionic radii ($\sim 0.474 \text{ nm}$). Sodium ions diffuse easily through these passages. The structure of $\text{Na}_4\text{V}_2(\text{PO}_4)_3$: contains two types of sites of Na cations: The type 1 lies within the $[\text{V}_2(\text{PO}_4)_3]$ unit along the c-direction, while three type 2 sites lie adjacent to P atoms having the same c-coordinate. The sites type 1 and two of three type 2 sites are completely occupied, enabling mobility of ions in type 2 sites.

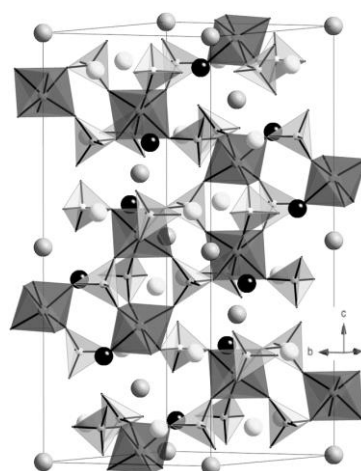


Figure 13. The crystal structure of NVP. The V ions are centers of octahedra (red) and the P ions are centers of tetrahedra (grey). Sodium ions at the Na_1 sites are designated by light balls, ions at Na_2 site are designated by gray balls and the empty Na sites are shown by black balls. [32] Copyright Royal Society of Chemistry

Wang et al [40] synthesized $\text{Na}_3\text{V}_2(\text{PO}_4)_3/\text{carbon}$ composite by a sol-gel method using citric acid as a gelling agent. Upon gel drying and carbonization a porous, carbon coated, crystals are obtained enabling highly conductive network and developed surface contacting with electrolyte solution. When used as cathode material excellent electrochemical performance was observed: superior high-rate capacity (78 mA h g^{-1} at 192 C , approaching 76.9% of the initial capability of 98.6 mA h g^{-1} at 0.5 C), high cycling stability (98.4% retention after 800 cycles at 1 C and 91.4% retention after 2000 cycles at 10 C), and 76.0% of capacity retention after 3000 cycles at 100 C .

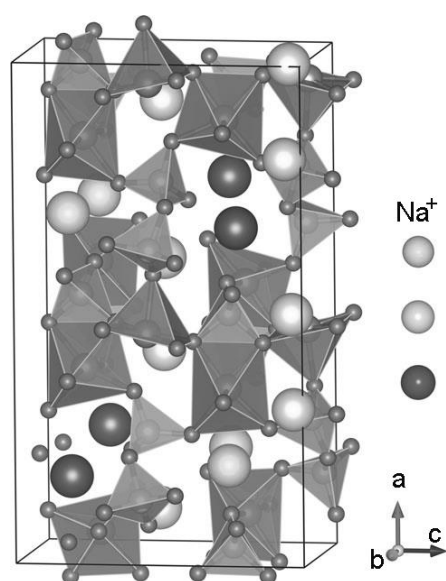


Figure 14. The structure of $\text{Na}_4\text{Fe}_3(\text{PO}_4)_2(\text{P}_2\text{O}_7)$. Various Na-ion sites are represented by large differently nuanced balls [41]



Recently, Chen et al. [41] found a new Fe-based polyanionic compound, $\text{Na}_4\text{Fe}_3(\text{PO}_4)_2(\text{P}_2\text{O}_7)$, which belongs to a class of NASICON-type materials. The obtained compound displayed a nanoplatelet form of tunable dimensions and a high degree of crystallinity. Its crystalline structure is shown in Figure 14. The $[\text{Fe}_3\text{P}_2\text{O}_{13}]$ units placed along the vertical a-axis of unit cell consist of three FeO_6 octahedra and three PO_4 groups; the $[\text{Fe}_3\text{P}_2\text{O}_{13}]_\infty$ units placed to form infinite layers are connected by $[\text{P}_2\text{O}_7]$ groups along the direction. This structure allows large primary tunnels along the b direction but is open for 3D diffusion of sodium ions. For the one-step sol-gel synthesis they used ethylenediaminetetraacetic acid (EDTA) as the complexing agent. During synthesis procedure, on heating in inert atmosphere, EDTA undergoes carbonization, producing an uniform carbon coating

around the crystalline particles. This coating enabled high electronic conductivity of the sample. This composite material was investigated in the electrolyte solution composed of ethylene carbonate/propylene carbonate solution (EC/PC, 1:1 by volume) and 1 M NaClO_4 to which 5 vol. \% fluoroethylene carbonate (FEC) was added. When used as cathode material of a battery, it exhibits an excellent capacity versus charging rate performances, 113.0 and 80.3 mAh g^{-1} at 0.05 C and 20 C , respectively. Also high cycling stability was observed without noticeable voltage fade (the coulombic capacity retention amounted to 69.1% after 4400 cycles at 20 C) with almost 100% efficiency. The air stability and all-climate ($-20 \text{ }^\circ\text{C}$ and $50 \text{ }^\circ\text{C}$) performance were also investigated. An excellent air stability and low influence of cooling at $-20 \text{ }^\circ\text{C}$ were evidenced (84.7 mAh g^{-1} at 0.2 C) A low-cost all-iron-based.

6. ANODE MATERIALS OF SODIUM – ION BATTERIES

Structurally disordered carbon

Zhou et al [42] obtained structurally disordered carbon by pyrolysis at $800 \text{ }^\circ\text{C}$ of an intimate mixture of soluble polymers poly(diallyldimethylammonium chloride) (PDDA) and poly(sodium 4-styrenesulfonate) (PSS). The spacing between the graphitic layers of 0.39 nm corresponds well to the ionic radius of sodium ion. This carbon type was used as electrode material in the electrolyte obtained from

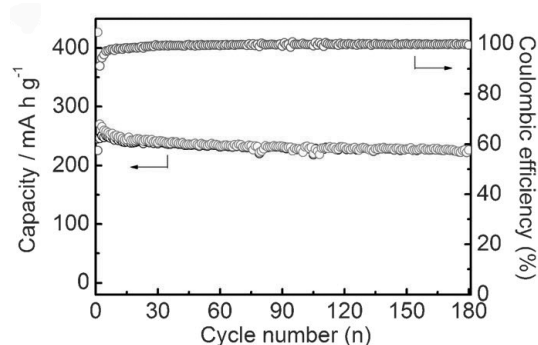


Figure 15. Specific capacity of highly disordered carbon versus cycle number Obtained at rate 100 mA/g . [42]

Copyright 1999-2020 by John Wiley & Sons Inc.

NaClO_4 (1M) dissolved in a solvent mixture propylene carbonate + ethylene carbonate, and superior cycling stability and rate capability were evidenced Figure 15. A reversible capacity of 225 mAh/g and a capacity retention of 92% are achieved at a current density of 100 mA/g after 180 cycles. The

charging and discharging occurs between 0 and 0.5 V vs metallic sodium.

Tin

Tin forms several intermetallic compounds with sodium, which may be obtained either by standard metallurgy methods or by cathodic deposition of sodium on finely dispersed tin in organic solution of sodium salt. Fully sodiated alloy has the composition $\text{Na}_{15}\text{Sn}_4$. The theoretical capacity of this compound is 847 mAh g^{-1} [43].

The main disadvantage of Sn anodes is a large volume expansion, which amounts to 420% for full transition from Sn to $\text{Na}_{15}\text{Sn}_4$ [44]. Such volume change disintegrates electrode layer and leads to a short cycle life. Various strategies were applied to remove this disadvantage.

Several attempts were reported by making composites with carbon, on account of reduction of available coulombic capacity of pure Sn [45,46]. Datta et al. [45] used also ball milling to made composite of 70 wt% Sn and 30 wt% graphite. This composite displayed capacity of 410 mA g^{-1} in 1st cycle desodiation, and an efficiency of 70% at a current rate of 50 mA g^{-1} . The prolongation of ball-milling synthesis of Sn/C composite improved substantially the cycle life. For instance, the time rise in ball-milling procedure from 5 minutes to 1 h, the capacity fade dropped from initial 3.6% to 0.7% loss per cycle [45].

Kim et al [46] by ball-milling of Sn with carbon nanotubes synthesized a three-dimensional porous coral-like composite of micrometer-sized Sn particles bonded mutually by room temperature sintering. The coral like structure manifested itself as mechanically stable during cyclic volume change caused by sodiation/desodiation. When used as anode with the composition 70 wt% Sn, 15 wt% polyvinylidene fluoride glue (PVDF), and 15 wt% multiwalled carbon nanotubes in 1 M NaPF₆ dissolved in 1,2-dimethoxyethane as electrolyte solution, this composite displayed capacity of 554 mA h g^{-1} at 10C-current rate for 5000 cycles, and nearly 100% capacity retention up to even 5000 cycles. It seems that this anode material displayed self-healing behavior helping so stable performance on long-term cycling.

Hu et al [47] deposited atomically thin Al_2O_3 layer over Sn nanoparticles to attach them on carbon nanofibers support. With the upper desodiation potential of 1.5 V, he evidenced high desodiation capacity of over 600 mAh g^{-1} , and very stable potential plateau by cycling for 40 cycles. Compared to Sn/C composite formation, this study

demonstrated alternative way to buffer volume change of Sn anode material on cycling.

Liu et al [48] studied the effect of conduction polymer glues on pure nanodispersed Sn anode on its electrochemical performance. With poly(9,9-dioctylfluorene-co-fluorenone-comethylbenzoic ester) (PFM) binder an initial desodiation capacity of 806 mAh g^{-1} , was found, with the efficiency $\sim 70\%$ at a current rate of C/50 (16 mA g^{-1}). Usual binders, carboxymethylcellulose (CMC) and PVDF enabled much lower capacities, 536 mAh g^{-1} and 65 mAh g^{-1} , respectively. The high capacity achieved by PFM binder was explained by ability of this binder to enhance conductivity and prevent detachment active mass from the support (Figure 16).

Hu et al., [49] reported that natural wood fibers may be used as a support that prevents disadvantages connected to the volume change of Sn on sodiation [49] and absorbing electrolyte help the ionic conductivity of anode material. The study demonstrated acceptable long-term cycling. Namely at a current rate of 85 mA g^{-1} the anode retained the coulombic capacity of 145 mAh g^{-1} upon 400 cycles.

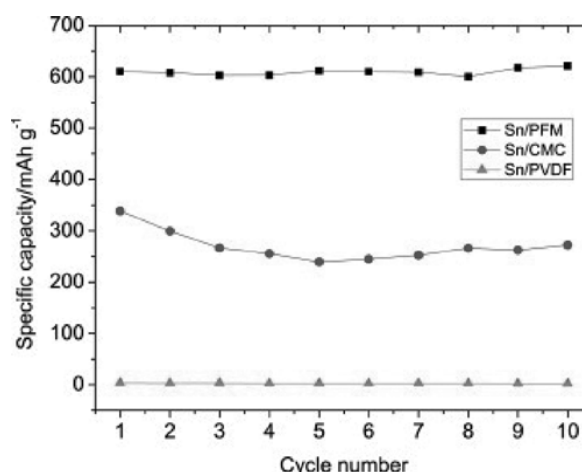


Figure 16. Comparison of coulombic capacity versus cycle number of a pure Sn/binder anode for different binders.

Current rate 16 mA g^{-1} [48] Copyright Elsevier 2014

Red phosphorous

Like to alloying with lithium, phosphorous using as anode material inorganic electrolyte solutions builds alloys with sodium up to the composition Na_3P . Theoretical gravimetric energy capacity corresponding to this composition amounts to 2596 mAh g^{-1} . Operating potential during sodiation and desodiation is around 0.4 V vs Na^+/Na electrode, which provides high-voltage of a full cell, and prevents the formation of metallic dendrites on cyclic polarization. Therefore, phosphorous attracted care and was broadly investigated as an anode material of alkali-ion batteries.

Qian et al. [50] found that the sodiation, i.e. transition from P to Na_3P is slow and needs to be performed at low current densities. This indicates formation of resistant surface layers during sodiation. On the contrary, transition from Na_3P to P is fast and not too sensitive to the current rate. The main disadvantages of red phosphorus as an electrode material are low conductivity and high volume expansions on sodiation. A volume expansion corresponding to the transition from P to Na_3P amounts to 308%. Both low conductivity and high volume expansion may be prevented by using composite P/C instead of pure phosphorus.

Kim et al. [51] synthesized red phosphorus/carbon composite powder by ball milling of commercially available amorphous red phosphorus and Super P carbon as a conducting additive. They reported that the optimal carbon fraction in P/C composite evaluated using coin cells with Na metal anode and electrolyte solution composed of 0.8 M NaClO_4 in ethylene carbonate and diethyl carbonate (1:1 v/v), is roughly 30% by mass. Namely, this material displayed a high desodiation capacity of 1540 mAh g^{-1} at a high current rate of even 2.86 A g^{-1} (roughly 1C rate), while 80% of the reversible capacity was measured at 143 mA g^{-1} (ca. 0.05C rate) [51]. The volume expansion of P/C composition with 30% C amounts to 187%, which is bearable in anode function, and provides reversible long-term cycling prospects. With lower carbon content, lower rate capabilities were evidenced. Chou et al. [52] found that the composite of red phosphorus with carbon nanotubes made by hand grinding displayed acceptable anode behavior, however, by prolonged grinding to 20 h the capacity of 862 mAh g^{-1} was observed, which maintained itself at the level of 73.5% after 50 cycles. Much better performance of this composite was published by Zhu et al. [53] upon fabrication modification. For P/SWCNT (single-walled carbon nanotubes) composite fabricated by the vaporization-condensation method, they found the capacity of $\sim 700 \text{ mAh g}^{-1}$ composite at a current density of 50 mA/g , high rate capability of $\sim 300 \text{ mAh g}^{-1}$ at even 2000 mA g^{-1} . Upon long-term cycling of 2000 sodiation-desodiation cycles, the capacity retention was 80%, which is 20 times higher than that observed with P/carbon composite obtained by milling.

7. CONCLUSIONS

In the early 1990s, a new type of battery, called lithium-ion battery, appeared as a commercial

product. It enabled four times higher energy density in comparison to classical predecessors. This battery prevailed on an expansively rising market of mobile electronics, and contributed to its massive development. In 2010, to prevent arising climate changes caused by consumption of fossil fuels, on the level of the Organization of United Nations, batteries obtained the role of power sources of electric cars with the intention to replace completely oil-powered vehicles till 2050. Recently, lithium-ion batteries received a third significant role in grid storage stabilization units, intended to stabilize output power of renewable energy sources. A rough forecast is that the rate of energy incorporation in batteries in 2030 will achieve 390 GWh per year. The significance of the invention of the lithium-ion battery was recognized by the Nobel Committee, which awarded the three scientists: S. Whittingham, J. Goodenough, and A. Yoshino, most meritorious for this invention, by the Nobel Prize in Chemistry in 2019. The expansion of the use of lithium-ion batteries in everyday life caused a huge increase in consumption of raw materials, lithium, cobalt, and nickel, the resources of which the latter two may be exhausted within the two next decades. In order to fulfill future global expectations from batteries in the field of both consumer electronics and environmental protection, new battery types should be developed. Based on the results of recent investigations, one of the real alternatives is the sodium ion battery. It works on the same principles as the lithium-ion one, but does not suffer from the problem of raw material abundance. Having in mind the recent development of perspective cathode and anode materials for sodium-ion batteries, namely 150 and more Ah kg^{-1} capacity withstanding thousands of charging/discharging cycles were published, there is a real perspective of commercial use of sodium-ion batteries at least in the area of grid storage. However, as the recent research results indicate, it is not excluded that their quality (energy density and cycle life) may achieve the values needed for mobile applications too.

8. ACKNOWLEDGEMENT

This work is supported by the Ministry of Education, Science and Technological Development of the Republic of Serbia (contract No. 451-03-9/2021-14/200146) and by the Serbian Academy of Sciences and Arts through the project F-190: Electrocatalysis in contemporary processes of energy conversion.

9. REFERENCES

- [1] X. Lu, G. Xia, J. P. Lemmon and Z. Yang, *Advanced materials for sodium-beta alumina batteries: Status, challenges and perspectives*, J. Power Sources, Vol. 195 (2010) 2431–2442.
- [2] W. Rüdorff, U. Hofmann, Über Graphitsalze, Z. Anorg. Allgem. Chemie, Vol. 238–1 (1938) 1–50.
- [3] A. Herold, *Insertion compounds of graphite with bromine and the alkali metals*, Bull. Soc. Chim. France, FR. (1955) 999.
- [4] E. Bayer, W. Rüdorff, *Reaction of Metalldisulfides having layer structures with alkaliphthalides-solutions*, Z. Naturforschung B, Vol. 27 (1972) 1336–1339.
- [5] M. S. Withingham, *The Role of Ternary Phases in Cathode Reactions*, J. Electrochem Soc., Vol. 123 (1976) 315.
- [6] M. M. Thackeray, W. I. F. David, P. G. Bruce, J. B. Goodenough, *Lithium insertion into manganese spinels*, Mater. Res. Bull., Vol. 18 (1983) 461–472.
- [7] M. G. S. R. Thomas, W. I. F. David, J. B. Goodenough and P. Groves, *Synthesis and structural characterization of the normal spinel $\text{Li}(\text{Ni}_2)\text{O}_4$* , Mat. Res. Bull., Vol. 20 (1985) 1137–1146.
- [8] J. R. Dahn, U. von Sacken, M. W. Juzkow and H. Al-Janaby, *Rechargeable $\text{LiNiO}_2/\text{Carbon Cells}$* , J. Electrochem Soc., Vol. 138 (1991) 2207–2211.
- [9] K. Mizushima, P. C. Jones, P. J. Wiseman, J. B. Goodenough, *Li_xCoO_2 ($0 < x < 1$): A new cathode material for batteries of high energy density*, Mat. Res. Bull., Vol. 15 (1980) 783–789.
- [10] A. Padhi, K. S. Nanjundaswamy, J. Goodenough, *Phospho-Olivines as Positive-Electrode Materials for Rechargeable Lithium Batteries*, J. Electrochem. Soc., Vol. 144 (1997) 1188–1194.
- [11] C. M. Julien, A. Mauger, K. Zaghib, H. Groult, *Comparative Issues of Cathode Materials for Li-Ion Batteries*, Inorganics, Vol. 2 (2014) 132–154.
- [12] R. Yazami, Ph. Touzain, *A reversible graphite-lithium negative electrode for electrochemical generators*, Journal of Power Sources, Vol. 9 (1983) 365–371.
- [13] A. Yoshino, K. Sanechika, T. Nakajima, *Secondary batteries*, USP4,668,595 and JP1989293, May 10, 1985 (Basic patent of the LIB.).
- [14] A. Yoshino, K. Nakanishi, A. Ono, *Explosion-proof secondary battery*, JP2642206, filing date December 28, 1989.
- [15] J. R. Dahn, U. von Sacken, M. W. Juzkow, H. Al-Janaby, *Rechargeable $\text{LiNiO}_2/\text{carbon cells}$* , J. Electrochem. Soc., Vol. 138 (1991) 2207–2201.
- [16] J. M. Tarascon, E. Wang, F. K. Shokoohi, W. R. McKinnon, S. Colson, *The spinel phase of LiMn_2O_4 as a cathode in secondary lithium cells*, J. Electrochem. Soc., Vol. 138 (1991) 2895–2864.
- [17] Z. Liu, A. Yu, J. Y. Lee, *Synthesis and characterization of $\text{LiNi}_{1-x-y}\text{Co}_x\text{Mn}_y\text{O}_2$ as the cathode materials of secondary lithium batteries*, J. Power Sources, Vol. 81–82 (1999) 416–419.
- [18] T. Ohzuku, Y. Makimura, *Layered lithium insertion material of $\text{LiCo}_{1/3}\text{Ni}_{1/3}\text{Mn}_{1/3}\text{O}_2$ for lithium-ion batteries*, Chem. Mater., Vol. 30 (2001) 642–643.
- [19] M. Guilmard, C. Poullerie, L. Croguennec, C. Delmas, *Structural and electrochemical properties of $\text{LiNi}_{0.70}\text{Co}_{0.15}\text{Al}_{0.15}\text{O}_2$* , Solid State Ionics, Vol. 160 (2003) 39–50.
- [20] K. J. Park, J. Y. Hwang, H. H. Ryu, F. Maglia, S. J. Kim, P. Lamp, C. S. Yoon and Y. K. Sun, *Degradation Mechanism of Ni-Enriched NCA Cathode for Lithium Batteries: Are Microcracks Really Critical?*, ACS Energy Lett., Vol. 4–6 (2019) 1394–1400.
- [21] D. D. MacNeil, Z. Lu, J. R. Dahn, *Structure and electrochemistry of $\text{Li}(\text{Ni}_x\text{Co}_{1-2x}\text{Mn}_x)\text{O}_2$ ($0 < x < 1/2$)*, J. Electrochem. Soc., Vol. 14 (2002) A1332–A1336.
- [22] N. Yabuuchi, T. Ohzuku, *Novel lithium insertion material of $\text{Li}(\text{Co}_{1/3}\text{Ni}_{1/3}\text{Mn}_{1/3})\text{O}_2$ for advanced lithium-ion batteries*, J. Power Sources, Vol. 119 (2003) 171–174.
- [23] I. Belharouak, Y. K. Sun, J. Liu, K. Amine, *$\text{Li}(\text{Co}_{1/3}\text{Ni}_{1/3}\text{Mn}_{1/3})\text{O}_2$ as a suitable cathode for high power applications*, J. Power Sources, Vol. 123 (2003) 247–252.
- [24] M. Vujković, I. Stojković, M. Mitrić, S. Mentus, N. Cvjetičanin, *Hydrothermal synthesis of $\text{Li}_4\text{Ti}_5\text{O}_{12}/\text{C}$ nanostructured composite: morphology and electrochemical performance*, Mat Res Bull., Vol. 48 (2013) 218–223.
- [25] M. Vujković, I. Stojković, N. Cvjetičanin, S. Mentus, *Gel-combustion synthesis of LiFePO_4/C composite with improved capacity retention in aerated aqueous electrolyte solution*, Electrochim. Acta, Vol. 92 (2013) 248–256.
- [26] M. Vujković, M. Mitrić, S. Mentus, *High-rate intercalation capability of $\text{NaTi}_2(\text{PO}_4)_3/\text{C}$ composite in aqueous lithium and sodium nitrate solutions*, J. Power Sources, Vol. 288 (2015) 176–186.
- [27] M. Vujković, I. Pašti, I. Stojković Simatović, B. Šljukić Paunković, M. Milenković, S.

Mentus, *The influence of intercalated ions on cyclic stability of V_2O_5 /graphite composite in aqueous electrolytic solutions: experimental and theoretical approach*, *Electrochim Acta*, Vol. 176 (2015) 130–140.

[28] M. Vujković, S. Mentus, *Potentiodynamic and galvanostatic testing of $NaFe_{0.95}V_{0.05}PO_4/C$ composite in aqueous $NaNO_3$ solution, and the properties of aqueous $Na_{1.2}V_3O_8/NaNO_3/NaFe_{0.95}V_{0.05}PO_4/C$ battery*, *J. Power Sources*, Vol. 325 (2016) 185–193.

[29] N. P. Diklić, A. Dobrota, I. A Pašti, S. V. Mentus, B. Johansson, N. V. Skorodumova, *Sodium storage via single epoxy group on graphene - The role of surface doping*, *Electrochimica Acta*, Vol. 297 (2019) 523–528.

[30] G. Zubi, R. Dufo-Lopez, M. Carvalho, G. Pasaoglu, *The lithium-ion battery: State of the art and future perspectives*, *Renew Sustain Energy Rew.*, Vol. 89 (2018) 292–308.

[31] K. Turcheniuk, D. Bondarev, V. Singhal, G. Yushin, *Ten years left to redesign lithium-ion batteries*, *Nature*, Vol. 559 (2018) 467–470.

[32] Website:
<http://www.nistep.go.jp/achiev/ftx/eng/stfc/stt039e/q r39pdf/STTqr3904.pdf>, accessed date: April, 2012.

[33] N. S. Choi, Z. Chen, S. A. Freunberger, X. Ji, Y. K. Sun, K. Amine, G. Yushin, L. F. Nazar, J. Cho, Peter G. Bruce, *Challenges Facing Lithium Batteries and Electrical Double-Layer Capacitors*, *Angew. Chem. Int. Ed.*, Vol. 51 (2012) 9994–10024.

[34] H. Pan, Y. S. Hu, L. Chen, *Room-temperature stationary sodium-ion batteries for large-scale electric energy storage*, *Energy Environ. Sci.*, Vol. 6 (2013) 2338–2360.

[35] W. J. Li, S. L. Chou, J. Z. Wang, Y. M. Kang, J. L. Wang, Y. Liu, Q. F. Gu, H. K. Liu, S. X. Dou, *Facile method to synthesize Na-enriched $Na_{1+x}FeFe(CN)_6$ frameworks as cathode with superior electrochemical performance for sodium-ion batteries*, *Chem. Mater.*, Vol. 27 (2015) 1997–2003.

[36] Y. You, X. L. Wu, Y. X. Yin and Y. G. Guo, *High-quality Prussian blue crystals as superior cathode materials for room-temperature sodium-ion batteries*, *Energy Environ. Sci.*, Vol. 7 (2014) 1643–1647.

[37] P. Xiao, J. Song, L. Wang, J. B. Goodenough, G. Henkelman, *Theoretical Study of the Structural Evolution of a $a_2FeMn(CN)_6$ Cathode upon Na Intercalation*, *Chem. Mater.*, Vol. 27 (2015) 3763–3768.

[38] Z. Shen, S. Guo, C. Liu, Y. Sun, Z. Chen, J. Tu et al., *Na-rich Prussian white cathodes for*

long-life sodium-ion batteries, *ACS Sustain. Chem. Eng.*, Vol. 6 (2018) 16121–16129.

[39] K. M. Bui, V. A. Dinh, S. Okada, T. Ohno, *Hybrid functional study of the NASICON-type $Na_3V_2(PO_4)_3$: crystal and electronic structures, and polaron–Na vacancy complex diffusion*, *Phys. Chem. Chem. Phys.*, Vol. 17–24 (2015) 30433–30439.

[40] E. Wang, M. Chen, X. Liu, Y. Liu, H. Guo, Z. Wu, et al., *Organic cross-linker enabling a 3D porous skeleton-supported $Na_3V_2(PO_4)_3$ /carbon composite for high power sodium-ion battery cathode*, *Small Methods*, Vol. 3 (2019) Art.No 1800169 (10 pages).

[41] M. Chen, W. Hua, J. Xiao, D. Cortie, W. Chen, E. Wang, et al., *NASICON-type air-stable and all-climate cathode for sodium-ion batteries with low cost and high-power density*, *Nat. Commun.*, Vol. 10 (2019) Art.No.1480.

[42] X. Zhou, Y. Guo Guo, *Highly disordered carbon as a superior anode material for room temperature sodium-ion batteries*, *ChemElectrochem*, Vol. 1 (2014) 83–86.

[43] L. Baggetto, P. Ganesh, R. P. Meisner, R. R. Unocic, J. C. Jumas, C. A. Bridges, G. M. Veith, *Characterization of sodium ion electrochemical reaction with tin anodes: Experiment and theory*, *J. Power Sources*, Vol. 234 (2013) 48–59.

[44] J. W. Wang, X. H. Liu, S. X. Mao, J. Y. Huang, *Microstructural Evolution of Tin Nanoparticles during In Situ Sodium Insertion and Extraction*, *Nano Lett.*, Vol. 12 (2012) 5897–5902.

[45] M. K. Datta, R. Epur, P. Saha, K. Kadakia, S. K. Park, P. N. Kuma, *Tin and graphite based nanocomposites: Potential anode for sodium ion batteries*, *J. Power Sources*, Vol. 225 (2013) 316–322.

[46] C. Kim, I. Kim, H. Kim, M. K. Sadan, H. Yeo, G. Cho, J. Ahn, J. Ahn and H. Ahn, *A self-healing Sn anode with an ultra-long cycle life for sodium-ion batteries*, *J. Mater. Chem. A*, Vol. 6 (2018) 22809–22818.

[47] X. Han, Y. Liu, Z. Jia, Y. C. Chen, J. Wan, N. Weadock, K. J. Gaskell, T. Li and L. Hu, *Atomic-Layer-Deposition Oxide Nanoglue for Sodium Ion Batteries*, *Nano Lett.*, Vol. 14–1 (2014) 139–147.

[48] K. Dai, H. Zhao, Z. Wang, X. Song, V. Battaglia, G. Liu, *Toward high specific capacity and high cycling stability of pure tin nanoparticles with conductive polymer binder for sodium ion batteries*, *J. Power Sources*, Vol. 263 (2014) 276–279.

[49] H. L. Zhu, Z. Jia, Y. C. Chen, N. Weadock, J. Y. Wan, O. Vaaland, X. G. Han, T. Li, L. B. Hu, *Tin anode for sodium-ion batteries using*

natural wood fiber as a mechanical buffer and electrolyte reservoir, Nano Lett., Vol. 13 (2013) 3093–3100.

[50] J. F. Qian, X. Y. Wu, Y. L. Cao, X. P. Ai, H. X. Yang, *High capacity and rate capability of amorphous phosphorus for sodium ion batteries*, Angew. Chem. Int. Ed., Vol. 52 (2013) 4633–4636

[51] Y. Kim, Y. Park, A. Choi, N. S. Choi, J. Kim, J. Lee, J. H. Ryu, S. M. Oh, and K. T. Lee, *An Amorphous Red Phosphorus/Carbon Composite as a Promising Anode Material for Sodium Ion Batteries*, Adv. Mater., Vol. 25 (2013) 3045–3049.

[52] W. Li, S. Chou, J. Wang, H. K. Liu, S. X. Dou, *Phosphorus and Carbon Nanotubes Composite As Anode for Sodium-Ion Batteries*, ECS Meeting Abstracts, Vol. MA2014-04, P1-Tuesday Poster Session.

[53] Y. Zhu, Y. Wen, X. Fan, T. Gao, F. Han, C. Luo, S. C. Liou, C. Wang, *Red phosphorus-single-walled carbon nanotube composite as a superior anode for sodium ion batteries*, ACS Nano., Vol. 9–3 (2015) 3254–3264.



УЛОГА БАТЕРИЈА У ЕНЕРГЕТИЦИ БЛИСКЕ БУДУЋНОСТИ

Сажетак: Од прве нафтне кризе почетком седамдесетих година, електрохемичари теже развоју хемијског извора енергије који је у стању да замени течна фосилна горива у саобраћају. Приметан успех постигнут је у деценији 1980–1990. Захваљујући новој класи материјала – интеркалатним једињењима, комерцијализована је нова батерија названа литијум-јонска батерија која има много већу густину енергије од својих претходника. У овом раду објашњено је порекло њене високе густине енергије. Појава нове батерије ефикасно је подржала ширење употребе и развој преносне електронике – мобилних телефона, преносних рачунара, таблета итд. Од 2010. године, у вези са глобалним намерама да се спрече климатске промене, батерије су добиле улогу извора енергије електричних аутомобила. Недавно, повезане са све већом употребом обновљивих извора енергије, за које је познато да имају променљив интензитет, батерије преузимају и улогу колектора енергије за потребе градске мреже, имајући функцију да ублажи промене мрежног напона. Све ово проузроковало је огроман пораст употребе батерија и поставља се питање о доступности глобалних ресурса литијума, кобалта и никла потребних за њихову производњу. Недавна прогноза је да ће ти ресурси бити врло брзо исцрпљени у деценији 2030–2040. Стога постоји снажна потреба за тражењем нових типова батерија, како би се барем делимично одржали расположиви ресурси литијума за захтевније примене. Као део решења која имају стварну перспективу, у току је развој натријум-јонске батерије. У том смислу разматрани су неки перспективни анодни и катодни материјали.

Кључне речи: климатске промене; интеркалатна једињења; литијум-јонска батерија; натријум-јонска батерија; светске резерве метала.



Paper received: 24 August 2020
Paper accepted: 30 September 2020